COMPARISON OF SIZING CALCULATIONS BASED ON EXERGY AND ELECTRIC POWER PRODUCTION FOR MOLTEN SALT THERMAL ENERGY STORAGE SYSTEMS

Odenthal C.*, Klasing F. and Bauer, T.
*Author for correspondence
Institute of Engineering Thermodynamics,
German Aerospace Center (DLR),
Linder Höhe, 51147 Cologne
Germany,
E-mail: christian.odenthal@dlr.de

ABSTRACT

In this work a fast numerical model for sizing calculations of thermocline with filler storage systems, implemented in Matlab®, is presented. With this model, two sizing approaches are used. The first approach is considered as the classic approach, based on regained exergy after a full storage cycle, whilst for the second approach, the storage model is coupled with a simplified solar field and power block model. In the latter case, produced electric power after a full storage cycle is used for the rating of the storage configurations. Both approaches show a high efficiency of the thermocline with filler system. The comparison of both approaches show the influence of fluctuating boundary conditions on the cyclic behavior of the storage system and eventually, its sizing results.

INTRODUCTION

High temperature thermal energy storage in liquid molten salts is a cost effective and proven technology for process heat and power plant applications [1]. Examples are the improved use of waste heat from industrial processes, enhancement of the flexibility of power stations and cogeneration, as well as the conversion and storage of fluctuating surplus electricity from renewable energy sources.

Some of the main advantages of molten salt technology are its high maturity, low costs for the storage material, high heat transfer rates and operation at ambient pressure levels. The thermocline concept promises further potential for cost reduction by storing hot and cold molten salt inside a single tank, separated due to density stratification. By embedding a low cost solid filler material into the molten salt storage tank, further cost reductions can be achieved [2]. A new test facility to investigate and advance this technology, namely “TESIS:store”, is currently being commissioned at DLR in Cologne.

Besides new technological challenges, originating mainly from chemical stability, the sizing of such dynamic systems has taken on greater significance. In most of the studies to the present date, sizing calculations are based on constant boundary conditions, which are derived from the connected energy source (i.e. solar field, industrial process) and energy sink (i.e. power block, industrial process). In reality, these boundary conditions are not constant. For example, during charging, the mass flow of the heat transfer fluid (HTF) is varying throughout the day and the time span of solar irradiation is different over the course of the year. Towards the end of the discharging period, the exit temperature of the storage volume will drop. Consequently, an attached power block will return a decreased HTF temperature back into the storage system. If the return temperature declines too far, the cold zone of the storage volume does so as well. In the subsequent charging cycle, the HTF coming from the storage volume now has a very low temperature. As a result, if the thermal power of the energy source is limited, the charging mass flow has to be reduced. These considerations show that boundary conditions have a significant impact on the operating behavior of such thermocline systems and it is therefore advisable to take them already into account during the sizing calculations.

NOMENCLATURE

d_{part}	[m]	particle diameter
h	[h]	Specific enthalpy
$\Delta E'_{\mathrm{stor,nom}}$	[W]	Initially available exergy
$\Delta E''_{\mathrm{stor}}$	[W]	Regained exergy during discharge
L_{stor}	[m]	Storage length
$\dot{m}$	[kg/s]	mass flow rate
m	[kg]	mass
T	[°C]	Temperature
ΔT_{e}	[K]	Permitted change in exit temperature
x	[m]	Cartesian axis direction
y	[m]	Cartesian axis direction
z	[m]	Cartesian axis direction
s	[J/kgK]	Specific entropy
t	[s]	time
t'_{e}	[s]	Storage time
v	[m/s]	velocity
V_{stor}	[m³]	storage volume
$\dot{Q}$	[W]	Thermal power
$\dot{Q}_f'''$	[W/m³]	Volumetric heat generation density
$\dot{Q}_{\mathrm{th}}$	[W]	Thermal power of the power block

Special characters

ε	[-]	Porosity
ρ	[kg/m³]	Density
Ξ	[-]	Exergy regain
Ψ	[-]	Electricity regain

Subscripts

f	fluid
s	solid
nom	nominal
set	set value

EXTERNAL BOUNDARY CONDITIONS

The computer model is based on the partial differential equations (PDE) of the temperature fields of the fluid and solid. For the fluid the transient term for the change in inner energy, the transport of thermal energy and the coupling with the solid are taken into account. Heat losses and conduction are neglected, since their influence is comparatively small, when considering large storage volumes being not on standby.

The fluid PDE then reads

$$\varepsilon \rho_f c_f \frac{\partial T_f}{\partial t} = -\rho_f c_f v_{0,x,f} \frac{\partial T_f}{\partial x} + \dot{Q}_f{}'''. \quad (1)$$

Here, ε denotes the porosity, $\rho_f c_f$ the volumetric heat capacity of the fluid, $v_{0,x,f}$ the superficial flow velocity of the fluid and $\dot{Q}_f{}'''$ the energy from or to the solid. In terms of the solid there is only the transient change in inner energy and a coupling term with the fluid, hence the solid PDE reads

$$(1-\varepsilon)\rho_s c_s \frac{\partial T_s}{\partial t} = \dot{Q}_s{}'''. \quad (2)$$

The product $\rho_s c_s$ is the volumetric heat capacity of the solid and $\dot{Q}_s{}'''$ the coupling term, where an effective heat transfer coefficient is used [3]. The film heat transfer coefficient is calculated from a Nusselt-correlation derived by Wakao et al. [4]. The pressure loss is calculated from Ergun's [5] equation.

To solve the PDEs, a spatial discretization is applied, leading to a set of ordinary differential equations (ODEs), which are discretized by an implicit scheme with respect to time. This leads to a system of linear dependent equations which can be described by

$$\bar{\bar{\boldsymbol{M}}} \cdot \boldsymbol{T}^{\mathbf{n+1}} = \boldsymbol{T}^{\mathbf{n}} + \boldsymbol{b}. \quad (3)$$

$\bar{\bar{\boldsymbol{M}}}$ is a sparse band matrix, $\boldsymbol{T}^{\mathbf{n+1}}$ and $\boldsymbol{T}^{\mathbf{n}}$ the vectors of the temperature field for the next and current time step, respectively, and vector $\boldsymbol{b}$ contains the boundary conditions. The linear system is solved by the Matlab® routine mldivide.

REFERENCE SCENARIO

For the present study, a solar thermal power plant is considered. The specifications for the heat source (i.e. solarfield) and the heat sink (i.e. power block) are given in the first part of Table 1. In the second part of Table 1, the specifications for the storage system are given.

Table 1: Input values for present study

Description	Value	Unit
Heat transfer fluid (HTF)	solarsalt	-
Storage time ($t'_{e,set}$)	8	h
Thermal power of the power block ($\dot{Q}_{th}$)	285	MW_{th}
Nominal mass flow power block ($\dot{m}_{f,nom}$)	918	kg/s
Nominal inlet temperature ($T'_{in,nom}$)	510	°C
Nominal outlet temperature ($T''_{in,nom}$)	310	°C
Storage material	basalt	-
Flow length storage volume (L_{stor})	variable	m
Permitted change in exit temperature (ΔT_e)	10; 50	K
Cross-sectional area (A_0)	600	m^2
Particle diameter (d_{part})	40	mm
Porosity (ε)	22	%
Permitted pressure loss (Δp_{max})	0.5	bar

To model the output of the solar field, data given by Hirsch et al. [6] has been adjusted to depict the qualitative progression of a solarsalt field. Since the mass flow is not constant, the charging period is adjusted, so that the equivalent of 8 full load hours of thermal energy during charging is achieved. The output data is given in Figure 1.

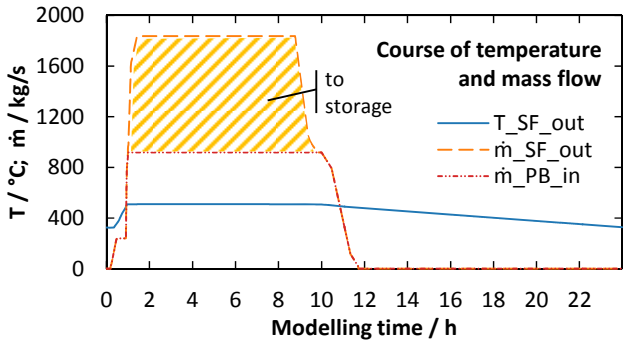

Figure 1: Course of temperature and mass flow of the solar field

For the heat sink, a solar thermal power block is used, which has been derived by Seitz [7]. The model uses HTF temperature and mass flow as input and returns gross electric power and HTF return temperature.

For the storage system, a thermocline filler system with low porosity is assumed. To achieve this, larger particles must be mixed with smaller ones. Since the larger particles are the limiting factor for heat transfer, the calculation is done with an assumed average particle diameter of 40 mm.

RATING APPROACHES

For the rating of the simulation results, two different approaches are considered.

Exergetic Rating

In the first approach, the nominal conditions given in Table 1 are used. These are taken as constant inlet conditions during charging and discharging. This can be considered as a classic approach for storage sizing, where the boundary conditions are derived from a specific system and assumed constant. Since the attached components are not modeled, a suitable measure for the storage performance is exergy E.

The actual rating methodology is based on an exergetic efficiency which can be regarded as an exergy regaining factor Ξ. Under nominal conditions, a specific exergy stream $\dot{E}'_{\mathrm{nom}}$ during the charging time t'_{e} is available. The resulting nominal exergy $\Delta E'_{\mathrm{stor,nom}}$ is fed into the storage volume and results in an extracted exergy $\Delta E''_{\mathrm{stor}}$ after discharging, as illustrated in Figure 2.

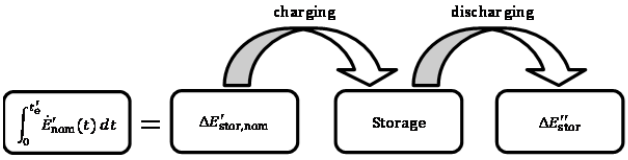

Figure 2: Exergetic quantities for the rating of the storage volume

The exergy regaining factor Ξ is defined as the quotient of extracted exergy $\Delta E''_{\mathrm{stor}}$ and the nominal exergy $\Delta E'_{\mathrm{stor,nom}}$, as given by the following equation

$$\Xi = \frac{\Delta E''_{\mathrm{stor}}}{\Delta E'_{\mathrm{stor,nom}}}, \tag{4}$$

where the initial exergy is calculated from

$$\Delta E'_{\mathrm{stor,nom}} = \int_0^{t'_{\mathrm{e}}} \dot{m}' \cdot \left[h\left(T'_{\mathrm{in,nom}}\right) - h\left(T'_{\mathrm{out,nom}}\right) - T_{\mathrm{u}} \cdot \left(s\left(T'_{\mathrm{in,nom}}\right) - s\left(T'_{\mathrm{out,nom}}\right)\right)\right] dt$$

and the regained exergy from

$$\Delta E''_{\mathrm{stor}} = \int_0^{t''_{\mathrm{e}}} \dot{m}'' \cdot \left[h\left(T''_{\mathrm{in,nom}}\right) - h\left(T''_{\mathrm{out}}(t)\right) - T_{\mathrm{u}} \cdot \left(s\left(T''_{\mathrm{in,nom}}\right) - s\left(T''_{\mathrm{out}}(t)\right)\right)\right] dt$$

In the equation, h denotes the specific enthalpy, s the specific entropy with 25°C as reference temperature und T_{u} the ambient temperature.

Rating Based on Electricity

In the second approach, the boundary conditions are not constant. During charging, the inlet temperature and mass flow is taken from the solarfield model. After 8 full load hours of energy is fed into the storage, the charging process is stopped and the storage is discharged. In this case, the nominal mass flow is used. As inlet temperature into the storage system, the HTF return temperature from the power block model is taken. Similar to the exergetic rating, the produced electricity from the storage system is based on the potentially producible electricity an expressed through the electricity regain factor Ψ.

RESULTS

As stated before, the permitted drop of the exit temperature has a vast impact on the utilization of the storage system. Figure 3 shows the temperature profiles over the length of the storage volume at the beginning and at the end of the charging process for the case with 50 Kelvin permitted change in exit temperature. As can be seen from Figure 4, if the permitted change in exit temperature is reduced to 10 Kelvin, the thermocline region runs significantly flatter than in the first case. The reason for this behaviour lies in the moment of switching from charging to discharging or vice versa. In this moment, there is a large temperature gradient between inflowing molten salt and the filler material. Due to this gradient, more heat can be transferred within a shorter section of the storage volume, reshaping the thermocline into a steeper progression.

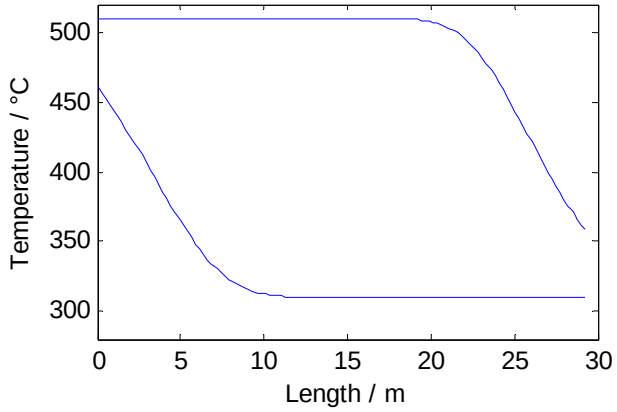

Figure 3: Temperature profile inside the storage volume at the beginning (lower curve) and end of the charging process (upper curve) for the case with constant boundary conditions and 50 Kelvin permitted change in exit temperature

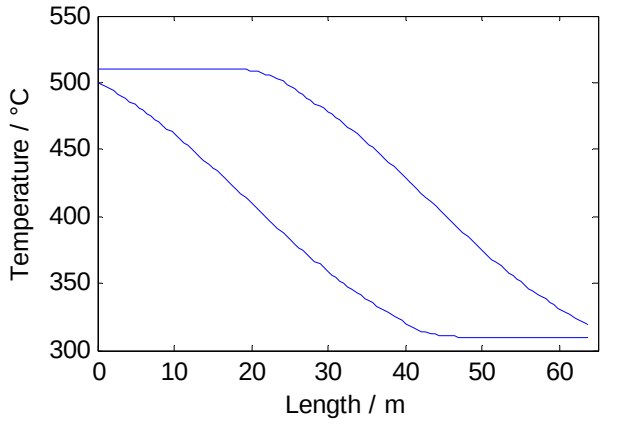

Figure 4: Temperature profile inside the storage volume at the beginning (lower curve) and end of the charging process (upper curve) for the case with constant boundary conditions and 10 Kelvin permitted change in exit temperature

Since the thermocline is thicker, it can also be seen from Figure 4, that the storage length has roughly doubled to maintain the specification of 8 hours charging time. The impact on storage size and exergy regain is summarized in Table 2. When comparing the thermocline system to the two-tank system, it should be noticed that the exergy regained from the storage is still very high with values not far from 100 %. The necessary fluid mass, however, can be significantly reduced. For the case with 50 Kelvin permitted temperature drop, only 7100 tons of molten salt are needed, instead of 26400 tons. Since molten salt contributes to roughly 50 % of the total capital costs of a two tank system [8], the thermocline with filler promises a huge cost reduction potential.

Table 2: Results for the exergetic rating and rating based on electricity for the thermocline filler system

System	**TC, exergetic**		**TC, electricity**		**2-T**	**-**
Permitted change in exit temperature (ΔT_e)	**10**	**50**	**10**	**50**	**0**	**K**
Exergy regain (Ξ)	98.6	97.5	-	-	100	%
Electr. regain (Ψ)	-	-	98.2	97.2	100	%
Storage length (L_{stor})	63.6	29.2	57	28.5	24.9	m
Storage volume (V_{stor})	38.2	17.5	34.2	17.1	15.0	$10^3 m^3$
Fluid mass (m_f)	15.4	7.1	13.8	6.9	26.4	kt
Solid mass (m_s)	89.0	40.1	79.8	39.9	0	kt

Next, Figure 5 shows the same temperature profiles at the beginning and end of the charging cycle, this time for the case with the solarfield and power block model. It can be seen, that there is a second drop of the initial temperature profile. The reason for that lies in the foregone discharging cycle. Towards the end of the discharging cycle, the exit temperature of the storage system drops. This has an impact on the power block as well. Figure 7 shows the electric power generation of the block which falls below 100 MW due to this temperature drop. Simultaneously, the temperature of the cold molten salt returning from the power block decreases as well.
Looking back on Figure 5, this second drop of the temperature at the cold end has again an impact on the next charging cycle. Since the thermal power of the solar field is fixed, the mass flow through the solar field has to be reduced. This means, that at the beginning of the next charging cycle, the storage system has to be charged at a lower mass flow rate, as shown in Figure 6.
Looking back on Table 2, the same conclusions as for the exergetic rating case can be drawn. Furthermore, a slight decrease of storage size can be noted, since the average temperature spreading is slightly increased.

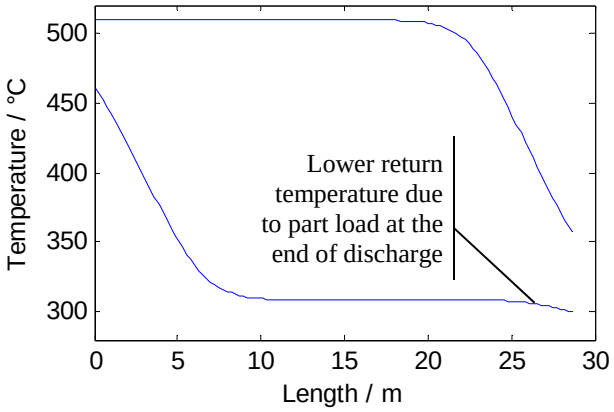

Figure 5: Temperature profile inside the storage volume at the beginning (lower curve) and end of the charging process (upper curve) for the case with variable boundary conditions

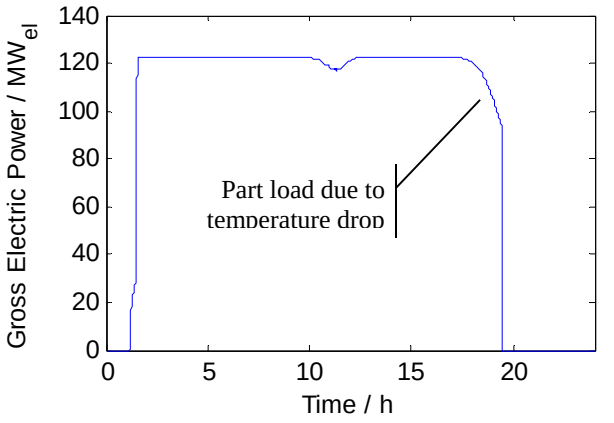

Figure 6: Gross electric power output and 50 Kelvin permitted temperature drop

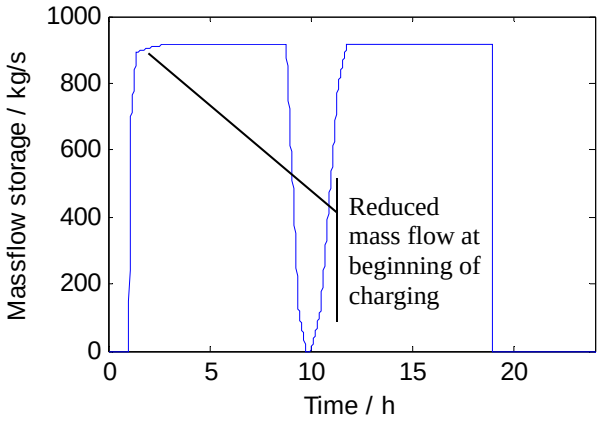

Figure 7: Mass flow for the storage system for the case with variable boundary conditions and 50 Kelvin permitted temperature drop

CONCLUSION

From the foregoing chapter, the following conclusions can be drawn.

- Permitted temperature drop has a vast impact on the utilization of the storage volume and should be maximized
- Thermocline storage with filler promises a huge cost reduction potential over the two tank system.
- Depending on the attached process, the return temperature to the storage volume should be considered. Especially, if the return temperature fluctuates widely, there is a notable impact in the storage system.
- The investigation of the storage system in conjunction with a power block model shows a high efficiency in terms of regainable electricity, similar to the exergetic rating approach. Hence, for comparisons, a purely exergetic rating appears suitable, but for cost calculations, electric power output appears more useful.

REFERENCES

[1] J. E. Pacheco, S. K. Showalter, and W. J. Kolb, “Development of a Molten-Salt Thermocline Thermal Storage System for Parabolic Trough Plants,” *J. Sol. Energy Eng.*, vol. 124, no. 2, p. 153, 2002.

[2] C. S. Libby, L. Cerezo, R. Bedilion, J. Pietruszkiewicz, M. Lamar, and R. Hollenbach, “Design of high temperature solar thermocline storage systems,” *SolarPaces Conf.*, pp. 3–6, 2010.

[3] F. W. Schmidt and A. J. Willmott, *Thermal energy storage and regeneration*, 1st ed. Washington, D.C., USA: Hemisphere Publishing Corporation, 1981.

[4] N. Wakao and S. Kagei, *Heat and mass transfer in packed beds*. New York: Gordon and Breach Science Publishers Inc., 1982.

[5] S. Ergun and a. a. Orning, “Fluid Flow through Randomly Packed Columns and Fluidized Beds,” *Ind. Eng. Chem.*, vol. 41, no. 6, pp. 1179–1184, Jun. 1949.

[6] T. Hirsch and H. Schenk, “Dynamics of oil-based Parabolic Trough plants - a detailed transient simulation model,” in *Proceedings of the SolarPACES 2010 conference*, 2010.

[7] M. Seitz, “Thermodynamische Simulation und Optimierung von Betriebszyklen bei solarthermischen Kraftwerken mit Flüssigsalzen als Wärmeträgermedien,” Hochschule Augsburg, 2012.

[8] U. Herrmann, B. Kelly, and H. Price, “Two-tank molten salt storage for parabolic trough solar power plants,” *Energy*, vol. 29, no. 5–6, pp. 883–893, 2004.